Inorg. Chem. **2006**, *45*, 5752–5759

Electron Spin–Spin Exchange Coupling Mediated by the Porphyrin π System

David A. Shultz,*,† Christopher P. Mussari,†,‡ Krishna Kumar Ramanathan,†,§ and Jeff W. Kampf||

Department of Chemistry, North Carolina State University, Raleigh, North Carolina 27695-8204, and Department of Chemistry, University of Michigan, Ann Arbor, Michigan 48109-1055

Received February 6, 2006

The syntheses and electron paramagnetic resonance (EPR) spectral characterizations of porphyrins (**1**–**3**) substituted with two radical groups bound to trans-meso positions are described. One of these compounds, **3**, has been studied by variable-temperature magnetic susceptibility and has been structurally characterized. Biradical porphyrin **3** is monoclinic, space group $P2_1/n$, with $a = 12.239(2)$ Å, $b = 17.819(3)$ Å, $c = 34.445(7)$ Å, $\alpha = 90°$, $\beta = 97.466(3)°$, $\gamma = 90°$, and $Z = 2$. The bis(nitroxide) porphyrins **1** and **2** exhibit fluid solution EPR spectra consistent with $|J| \gg |a|$. No evidence was observed for conformational modulation of J by rotation about single bonds as shown by the lack of change of the EPR spectra as a function of temperature. The bis(semiquinone) porphyrin **3** exhibits frozen-solution EPR spectra with zero-field splitting and a $\Delta m_s = 2$ transition characteristic of a triplet state. The intensity of the $\Delta m_s = 2$ transition of **3** was measured as a function of temperature, and the data fit according to a singlet–triplet model to yield J(**3**,solution) $= -75$ cm^{-1} ($H = -2J\hat{S}_1 \cdot \hat{S}_2$). Polycrystalline samples of porphryin **3** were examined by variable-temperature magnetometry. The paramagnetic susceptibility data were fit using a modified Bleaney–Bowers equation to give J(**3**,solid) $= -29$ cm^{-1} ($H = -2J\hat{S}_1 \cdot \hat{S}_2$). The antiferromagnetic J values are consistent with the π topology of the porphyrin ring.

Introduction

Open-shell molecular assemblies featuring metalloporphyrins are promising components of molecule-based magnetic materials.[1−25] In addition, porphyrins offer versatile frameworks for the construction of novel high-spin molecules. Along these lines, Iwamura and Koga prepared free-

* To whom correspondence should be addressed. Tel: (919) 515-6972. Fax: (919) 515-8920. E-mail: david_shultz@ncsu.edu. Web: http://www.ncsu.edu/chemistry/das.html

† North Carolina State University.

‡ Current address: Bristol-Myers Squibb, Pharmaceutical Research Institute, Princeton, NJ.

§ Current address: Senior Research Scientist, CiVenti Chem, Pittsboro, NC.

|| University of Michigan.

(1) Miller, J. S.; Calabrese, J. C.; McLean, R. S.; Epstein, A. J. *Adv. Mater.* **1992**, *4*, 498−501.
(2) Miller, J. S.; Vazquez, C.; Jones, N. L.; McLean, R. S.; Epstein, A. J. *J. Mater. Chem.* **1995**, *5*, 707−711.
(3) O'Shea, D. F.; Miller, M. A.; Matsueda, H.; Lindsey, J. S. *Inorg. Chem.* **1996**, *35*, 7325−7388.
(4) Bohm, A.; Vazquez, C.; McLean, R. S.; Calabrese, J. C.; Kalm, S. E.; Manson, J. L.; Epstein, A. J.; Miller, J. S. *Inorg. Chem.* **1996**, *35*, 3083−3088.
(5) Sugiura, K.; Arif, A. M.; Rittenberg, D. K.; Schweizer, J.; Ohrstrom, L.; Epstein, A. J.; Miller, J. S. *Chem.—Eur. J.* **1997**, *3*, 138−142.
(6) Girtu, N. A.; Wynn, C. M.; Sugiura, K.-I.; Miller, J. S.; Epstein, A. J. *Synth. Met.* **1997**, *85*, 1703−1704.
(7) Wynn, C. M.; Girtu, M. A.; Brinckerhoff, W. B.; Sugiura, K.-I.; Miller, J. S.; Epstein, A. J. *Chem. Mater.* **1997**, *9*, 2156−2163.
(8) Yates, M. L.; Arif, A. M.; Manson, J. L.; Kalm, B. A.; Burkhart, B. M.; Miller, J. S. *Inorg. Chem.* **1998**, *37*, 840−841.
(9) Brandon, E. J.; Arif, A. M.; Burkhart, B. M.; Miller, J. S. *Inorg. Chem.* **1998**, *37*, 2792−2798.
(10) Brandon, E. J.; Rittenberg, D. K.; Arif, A. M.; Miller, J. S. *Inorg. Chem.* **1998**, *37*, 3376−3384.
(11) Rittenberg, D. K.; Sugiura, K.; Arif, A. M.; Sakata, Y.; Incarvito, C. D.; Rheingold, A. L.; Miller, J. S. *Chem.—Eur. J.* **2000**, *6*, 1811−1819.
(12) Sugiura, K.; Ushiroda, K.; Johnson, M. T.; Miller, J. S.; Sakata, Y. *J. Mater. Chem.* **2000**, *10*, 2507−2514.
(13) Sugiura, K.; Mikami, S.; Johnson, M. T.; Raebiger, J. W.; Miller, J. S.; Iwasaki, K.; Okada, Y.; Hino, S.; Sakata, Y. *J. Mater. Chem.* **2001**, *11*, 2152−2158.
(14) Conklin, B. J.; Sellers, S. P.; Fitzgerald, J. P.; Yee, G. T. *Adv. Mater.* **1994**, *6*, 836.
(15) Griesar, K.; Athanassopoulou, M. A.; Bustamante, E. A. S.; Tomkowicz, Z.; Zaleski, A. J.; Haase, W. *Adv. Mater.* **1997**, *9*, 45−48.
(16) Koizumi, K.; Shoji, M.; Kitagawa, Y.; Taniguchi, T.; Kawakami, T.; Okumura, M.; Yamaguchi, K. *Polyhedron* **2005**, *24*, 2720−2725.
(17) Ikeue, T.; Furukawa, K.; Hata, H.; Aratani, N.; Shinokubo, H.; Kato, T.; Osuka, A. *Angew. Chem., Int. Ed.* **2005**, *44*, 6899−6901.
(18) Dawe, L. N.; Miglioi, J.; Turnbow, L.; Tallaferro, M. L.; Shum, W. W.; Bagnato, J. D.; Zakharov, L. N.; Rheingold, A. L.; Arif, A. M.; Fourmigue, M.; Miller, J. S. *Inorg. Chem.* **2005**, *44*, 7530−7539.
(19) Nakazawa, Y.; Hoffman, W.; Miller, J. S.; Sorai, M. *Solid State Commun.* **2005**, *135*, 71−76.
(20) Girtu, M. A. *J. Opt. Adv. Mater.* **2002**, *4*, 85−92.

10.1021/ic060209z CCC: $33.50
Published on Web 06/17/2006

Scheme 1

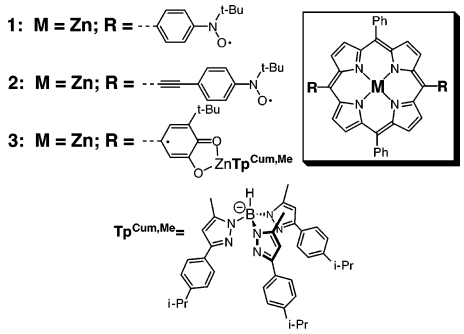

base and metalloporphyrins with one to four phenylcarbene groups that coupled with each other and with copper(II) bound in the porphyrin macrocycle.[26,27] Kamachi reported verdazyl-substituted porphyrins attached to polymer backbones.[28] Iwamura and others have also studied the magnetic behavior of pyridine nitroxides coordinated to chromium(III) tetraphenylporphyrin.[29,30] Recently, several doubly oxidized porphyrin dimers have been prepared that exhibit exchange coupling.[31−35]

Our efforts have focused on preparing new porphyrins as building blocks for coordination polymers and complexes with interesting magnetic or magneto-optic properties.[31,32,36−38] Herein, we describe the syntheses and electron paramagnetic resonance (EPR) spectral characterizations of porphyrins **1**−**3** (Scheme 1), which have stable nitroxide and stable semiquinone (SQ) complexes covalently attached to trans-meso positions of the porphyrin ring. One of these compounds, **3**, has been structurally characterized.

Results and Discussion

Synthesis. The syntheses of porphyrins **1**−**3** are shown in Scheme 2. Dibromoporphyrin **4**[39] was subjected to Suzuki

Scheme 2

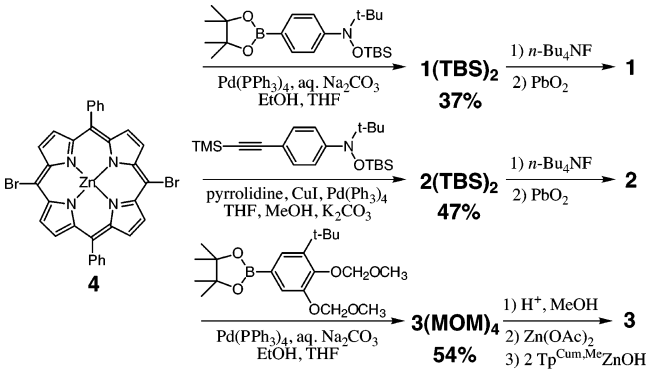

couplings to give **1(TBS)$_2$** and **3(MOM)$_4$** or to a modified Sonogashira coupling[31,40] to give **2(TBS)$_2$** (TBS = *tert*-butyldimethylsilyl; MOM = methoxymethyl). The syntheses of the boronic esters and alkyne used in the couplings have been reported previously.[38,41] Deprotection of the TBS groups of **1(TBS)$_2$** and **2(TBS)$_2$** was accomplished using tetra-*n*-butylammonium fluoride, and the corresponding hydroxylamines were immediately oxidized to the bis(nitroxide) biradicals using PbO_2 as described previously.[38]

The methoxymethyl-protected (MOM-protected) porphyrin **3(MOM)$_4$** was reacted with catalytic concentrated aqueous HCl in methanol to yield the corresponding bis(catechol) porphyrin and remetalated using zinc acetate. The metalated bis(catechol) porphyrin was reacted with 2 equiv of $Tp^{Cum,Me}$-ZnOH {$Tp^{Cum,Me}$ = hydro-tris[3(5)-cumenyl-5(3)-methylpyrazolyl]borate} to yield the corresponding bis(semiquinone) complex.[42−45] The formation of SQs is supported by EPR spectroscopy and by X-ray crystallography. Attempts to prepare X-ray quality crystals of both **1** and **2** were unsuccessful.

Molecular Structure of 3. An ORTEP of **3** is shown in Figure 1. Bond lengths for the dioxolene units are consistent with the SQ oxidation state as opposed to catecholate or protonated catecholate.[46,47] The SQ torsion angles with respect to the plane of the porphyrin ring are 58°, allowing moderate delocalization of the SQ spin density into the π system of the porphyrin. All other structural features are listed in the Supporting Information.

(21) Falk, K.; Haase, W. *Phys. Status Solidi A* **2002**, *189*, 979−982.
(22) Ostrovsky, S.; Haase, W.; Drillon, M.; Panissod, P. *Phys. Rev. B: Condens. Matter Mater. Phys.* **2001**, *64*, 134418−1−7.
(23) Falk, K.; Balanda, M.; Tomkowicz, Z.; Mascarenhas, F.; Schilling, J.; Klavins, P.; Haase, W. *Polyhedron* **2001**, *20*, 1521−1524.
(24) Mascarenhas, F.; Falk, K.; Klavins, P.; Schilling, J. S.; Tomkowicz, Z.; Haase, W. *J. Magn. Magn. Mater.* **2001**, *231*, 172−178.
(25) Johnson, M. T.; Arif, A. M.; Miller, J. S. *Eur. J. Inorg. Chem.* **2000**, 1781−1787.
(26) Iwamura, H. *Adv. Phys. Org. Chem.* **1990**, *26*, 179.
(27) Koga, N.; Iwamura, H. *Nippon Kagaku Kaishi* **1989**, 1456.
(28) Kamachi, M. *Nippon Butsuri Gakkaishi* **1987**, *42*, 351.
(29) Kitano, M.; Ishimaru, Y.; Inoue, K.; Koga, N.; Iwamura, H. *Inorg. Chem.* **1994**, *33*, 6012.
(30) Kitano, M.; Koga, N.; Iwamura, H. *J. Chem. Soc., Chem. Commun.* **1994**, 447.
(31) Shultz, D. A.; Lee, H.; Gwaltney, K. P. *J. Org. Chem.* **1998**, *63*, 7584−7585.
(32) Shultz, D. A.; Lee, H.; Gwaltney, K. P.; Sandberg, K. A. *Mol. Cryst. Liq. Cryst.* **1999**, *334*, 459−467.
(33) Nakazaki, J.; Senshu, Y.; Segawa, H. *Polyhedron* **2005**, *24*, 2538−2543.
(34) Segawa, H.; Senshu, Y.; Nakazaki, J.; Susumu, K. *J. Am. Chem. Soc.* **2004**, *126*, 1354−1355.
(35) Segawa, H.; Machida, D.; Senshu, Y.; Nakazaki, J.; Hirakawa, K.; Wu, F. P. *Chem. Commun.* **2002**, 3032−3033.
(36) Shultz, D. A.; Knox, D. A.; Morgan, L. W.; Sandberg, K.; Tew, G. N. *Tetrahedron Lett.* **1993**, *34*, 3975−3978.
(37) Shultz, D. A.; Sandberg, K. A. *J. Phys. Org. Chem.* **1999**, *12*, 10−18.
(38) Shultz, D. A.; Gwaltney, K. P.; Lee, H. *J. Org. Chem.* **1998**, *63*, 769−774.
(39) LeCours, S. M.; Guan, H.-W.; DiMagno, S. G.; Wang, C. H.; Therien, M. J. *J. Am. Chem. Soc.* **1996**, *118*, 1497−1503.
(40) Shultz, D. A.; Gwaltney, K. P.; Lee, H. *J. Org. Chem.* **1998**, *63*, 4034−4038.
(41) Shultz, D. A.; Boal, A. K.; Driscoll, D. J.; Farmer, G. T.; Hollomon, M. G.; Kitchin, J. R.; Miller, D. B.; Tew, G. N. *Mol. Cryst. Liq. Cryst.* **1997**, *305*, 303−310.
(42) Ruf, M.; Noll, B. C.; Groner, M. D.; Yee, G. T.; Pierpont, C. G. *Inorg. Chem.* **1997**, *36*, 4860−4865.
(43) Shultz, D. A.; Bodnar, S. H. *Inorg. Chem.* **1999**, *38*, 591−594.
(44) Shultz, D. A.; Bodnar, S. H.; Kampf, J. W. *Chem. Commun.* **2001**, 93−94.
(45) Shultz, D. A.; Fico, R. M., Jr.; Bodnar, S. H.; Kumar, R. K.; Vostrikova, K. E.; Kampf, J. W.; Boyle, P. D. *J. Am. Chem. Soc.* **2003**, *125*, 11761−11771.
(46) Shultz, D. A.; Bodnar, S. H.; Kumar, R. K.; Lee, H.; Kampf, J. W. *Inorg. Chem.* **2001**, *40*, 546−549.
(47) Pierpont, C. G.; Buchanan, R. M. *Coord. Chem. Rev.* **1981**, *38*, 45−87.

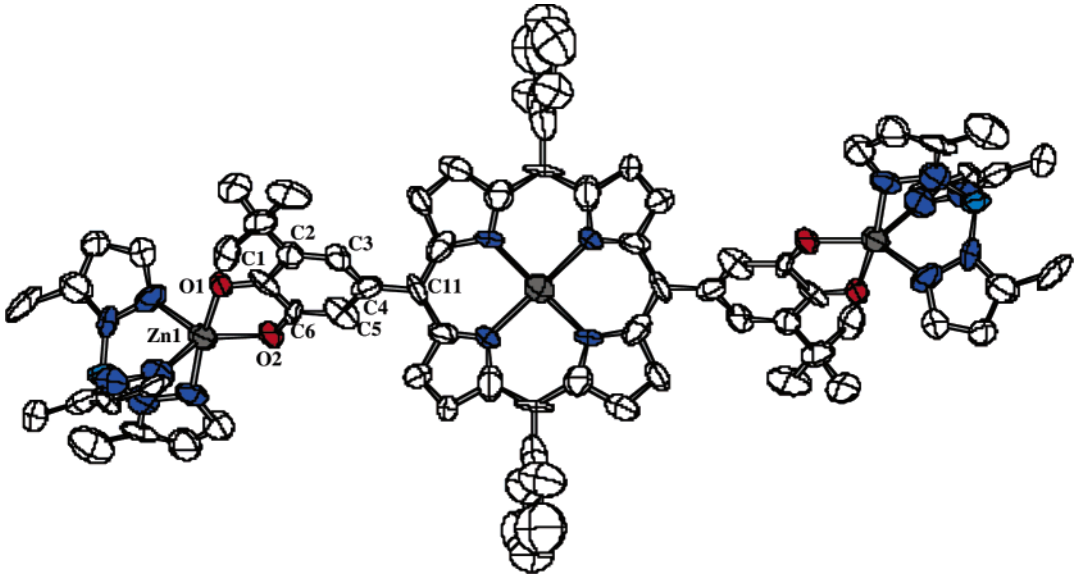

Figure 1. ORTEP of bis(SQ) porphyrin, **3**; monoclinic $P2_1/n$, $a = 12.239(2)$ Å, $b = 17.819(3)$ Å, $c = 34.445(7)$ Å, $\alpha = 90°$, $\beta = 97.466(3)°$, $\gamma = 90°$, and $Z = 2$. Data collected at 158 K. Solvent molecules, hydrogens, and cumenyl groups have been omitted for clarity.

Table 1. Bond Lengths (Å) for SQ Rings of **3**

Zn(1)-O(2)	1.952(10)
Zn(1)−O(1)	2.134(10)
O(1)−C(1)	1.243(17)
O(2)−C(6)	1.260(19)
C(1)−C(2)	1.48(2)
C(1)−C(6)	1.50(2)
C(2)−C(3)	1.356(18)
C(3)−C(4)	1.456(19)
C(4)−C(5)	1.41(2)
C(4)−C(11)	1.45(2)
C(5)−C(6)	1.38(2)

Bis(nitroxide) Porphyrins 1 and 2. Several years ago, we reported the preparation and EPR spectral characterization of three nitroxide-substituted porphyrins shown in Figure 2 (Mes = mesityl, 2,4,6-trimethylphenyl).[38] One of our goals is to maximize spin delocalization into the porphyrin to achieve the maximum exchange coupling with bound paramagnetic metal ions. We recognized that direct attachment of the phenylnitroxide to the porphyrin would result in substantial phenyl torsion[48] that would attenuate delocalization.[45,49] The addition of a spacer group (e.g., −CH═CH− or −C≡C−) would dilute the spin density but would allow for greater coplanarity of phenylnitroxide and porphyrin rings, hopefully increasing the spin delocalization despite spin dilution. Thus, assessing spin-delocalization-limiting torsion versus spin-delocalization-promoting coplanarity is critical for evaluating design principles for high-spin molecules based on porphyrins.[45,49]

Previously, we could not easily distinguish differences in spin delocalization as a function of nitroxide functionality,[38] and we hoped that the EPR spectral characterization of **1** and **2** could answer the question of which functionality resulted in the greatest spin delocalization into the porphyrin π system.

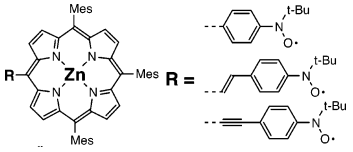

Figure 2. Mononitroxide Zn^{II} porphyrins studied previously.

We reasoned that exchange coupling could be quite weak in biradicals **1** and **2**, and J might be strongly modulated (and modulated differentially in **1** and **2**) by C_{meso}−C bond torsion (C_{meso} is the porphyrin *meso*-carbon; C is the carbon of the nitroxide functionality: a phenyl carbon in **1** and an ethyne carbon in **2**), and the alternating line-width effect might be observed.[50−52] However, as shown in Figures 3 and 4, the EPR spectral shapes of both **1** and **2**, respectively, are temperature-invariant between ca. 250 and 365 K, suggesting that (1) $|J| \gg |a|$ at all torsion angles and (2) bond rotation is extremely fast at all of the temperatures studied. The second point is most likely for **2** because phenyl torsions in phenylalkynes have extremely small torsional barriers of ca. 0.6 kcal/mol.[53,54] For **1**, the barrier is expected to be larger than that for **2**,[55] such that J modulation might be more reasonable for **1**. However, the invariance of the fluid-solution EPR spectral shape of **1** with temperature is consistent with the fact that $|J| \gg |a|$ regardless of the phenylnitroxide torsion angles. This is reasonable because $|J|$ need only be greater than ca. 10^{-3} cm^{-1}, the value of the N-hyperfine interaction.

The frozen-solution EPR spectra of **1** and **2** are typical for dinitroxides having small D values and N-hyperfine

(48) Scheidt, W. R.; Lee, Y. J. Recent Advances in the Stereochemistry of Metallotetrapyrroles. In *Structure and Bonding*; Buchler, J. W., Ed.; Springer-Verlag: Berlin, 1987; Vol. 64, pp 1−70.
(49) Shultz, D. A.; Fico, R. M., Jr.; Lee, H.; Kampf, J. W.; Kirschbaum, K.; Pinkerton, A. A.; Boyle, P. D. *J. Am. Chem. Soc.* **2003**, *125*, 15426−15432.
(50) Luckhurst, G. R. *Mol. Phys.* **1966**, *10*, 543−550.
(51) Glarum, S. H.; Marshall, J. H. *J. Chem. Phys.* **1967**, *47*, 1374−1378.
(52) Hudson, A.; Luckhurst, G. R. *Chem. Rev.* **1969**, *69*, 191−225.
(53) Okuyama, K.; Hasagawa, T.; Ito, M.; Mikami, N. *J. Phys. Chem.* **1984**, *88*, 1711−1716.
(54) Bothner-By, A. A.; Dadok, J.; Johnson, T. E.; Lindsey, J. S. *J. Phys. Chem.* **1996**, *100*, 17551−17557.
(55) Noss, L.; Liddell, P.; Moore, A.; Moore, T.; Gust, D. *J. Phys. Chem. B* **1997**, *101*, 458−465.

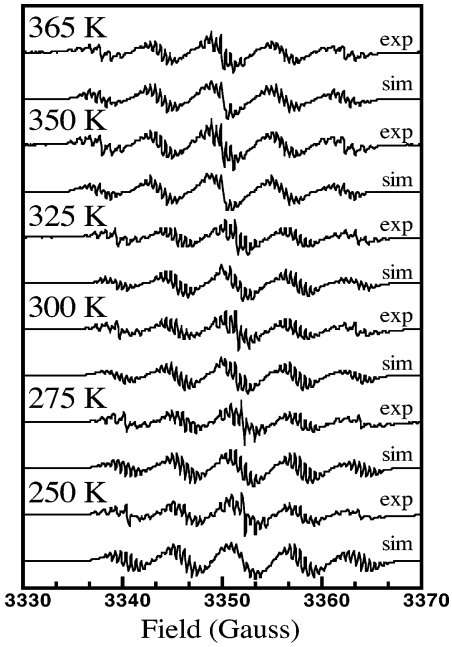

Figure 3. X-band fluid solution (1 mM in toluene) EPR spectra and simulations of **1** at different temperatures.

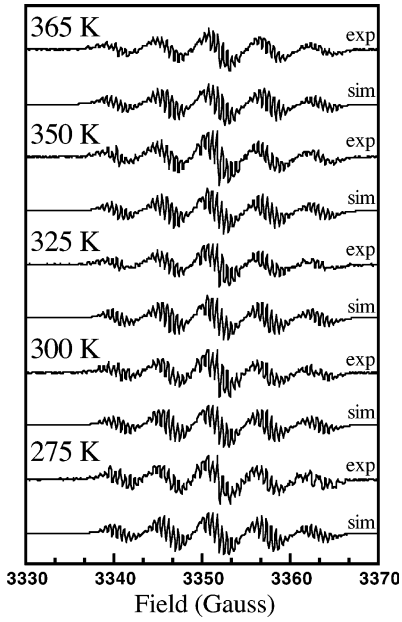

Figure 4. X-band fluid solution (1 mM in toluene) EPR spectra and simulations of **2** at different temperatures.

structure in the $\Delta m_s = 1$ region.[56−60] These spectral features, unfortunately, preclude our simulating the spectra to extract pertinent spin Hamiltonian parameters. However, both **1** and **2** exhibit very weak $\Delta m_s = 2$ features near half-field, indicating that dipole−dipole interactions are quite weak because the intensity of this feature is proportional to the zero-field-splitting parameter, D.[61] Therefore, we cannot distinguish exchange coupling in **1** from exchange coupling in **2** using EPR spectroscopy.

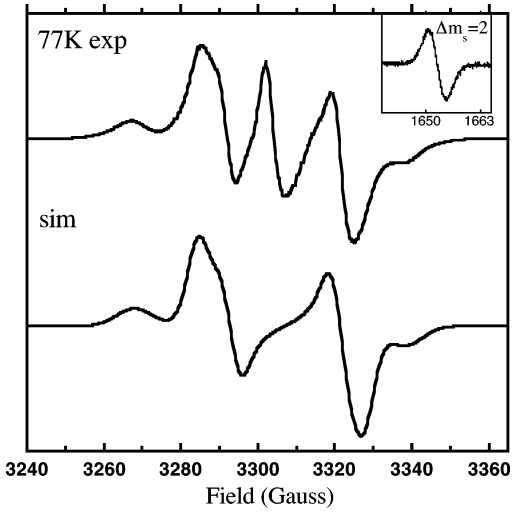

Figure 5. X-band frozen solution (10 mM solutions in toluene) EPR spectra of biradical **3** (top, experimental; bottom, simulation). Inset: $\Delta m_s = 2$ transition.

Bis(semiquinone) Porphyrin 3. Pierpont et al. reported the reaction of $Tp^{Cum,Me}ZnOH$ with (tetrahydroxyphthalocyaninato)nickel(II), a reaction that did not result in semiquinone formation.[62] Instead, monodentate and weakly coordinated bidentate complexes of $Tp^{Cum,Me}Zn^+$ with the catechol-like OH groups of (tetrahydroxyphthalocyaninato)-nickel(II) were formed. The formation of semiquinone complexes in the present cases is consistent with the weaker electron withdrawing character of the porphyrin ring system compared to that of a phthalocyanine ring system. The greater electron withdrawing capacity of a phthalocyanine, therefore, should require an oxidizing agent stronger than oxygen to complete the formation of the semiquinone complex. The lack of IR stretching near 1660 cm^{-1} (quinone) and 1250 cm^{-1} (catecholate) for **3** suggests the presence of semiquinone groups.

Positive evidence for the presence of SQ groups comes from EPR spectroscopy. The fluid-solution EPR spectrum consists of single broad lines lacking hyperfine structure. However, as shown in Figure 5, the frozen-solution EPR spectrum recorded at 77 K exhibits fine structure characteristic of a triplet state.[63−65] Also observable near half-field is a $\Delta m_s = 2$ transition (Figure 5, Inset). Both of these observations are consistent with an $S = 1$ bis(SQ) biradical. Simulation[66] of the $\Delta m_s = 1$ region of the EPR spectrum of **3** gives zero-field-splitting parameters $|D/hc| = 0.0033$ cm^{-1}

(56) Mitsumori, T.; Inoue, K.; Koga, N.; Iwamura, H. *J. Am. Chem. Soc.* **1995**, *117*, 2467−2478.
(57) Matsumoto, T.; Ishida, T.; Koga, N.; Iwamura, H. *J. Am. Chem. Soc.* **1992**, *114*, 9952−9959.
(58) Matsumoto, T.; Koga, N.; Iwamura, H. *J. Am. Chem. Soc.* **1992**, *114*, 5448−5449.
(59) Akita, T.; Mazaki, Y.; Kobayashi, K.; Koga, N.; Iwamura, H. *J. Org. Chem.* **1995**, *60*, 2092−2098.
(60) Shultz, D. A.; Boal, A. K.; Lee, H.; Farmer, G. T. *J. Org. Chem.* **1999**, *64*, 4386-4396.
(61) Weissman, S. I.; Kothe, G. *J. Am. Chem. Soc.* **1975**, *97*, 2537−2538.
(62) Ruf, M.; Lawrence, A. M.; Noll, B. C.; Pierpont, C. G. *Inorg. Chem.* **1998**, *37*, 1992−1999.
(63) Wasserman, E.; Snyder, L. C.; Yager, W. A. *J. Chem. Phys.* **1964**, *41*, 1763−1772.
(64) Atherton, N. M. *Principles of Electron Spin Resonance*; Ellis Horwood PTR Prentice Hall: New York, 1993.
(65) Wertz, J. E.; Bolton, J. R. *Electron Spin Resonance*; Chapman and Hall: New York, 1986.
(66) *WINEPR SimFonia*, v. 1.25, Shareware Version ed.; Brüker Analytische Messtechnik GmbH: Rheinstetten, Germany, 1996.

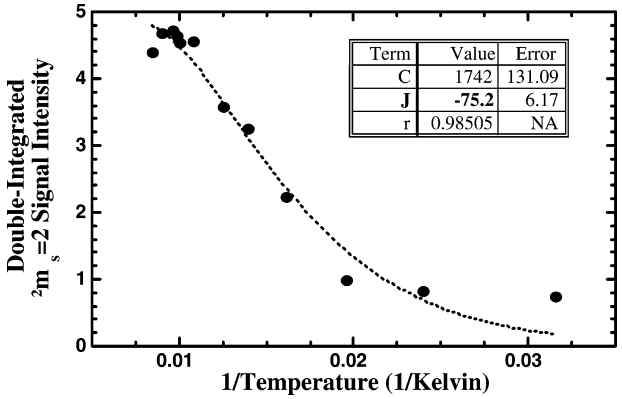

Figure 6. EPR Curie plot for biradical **3**.

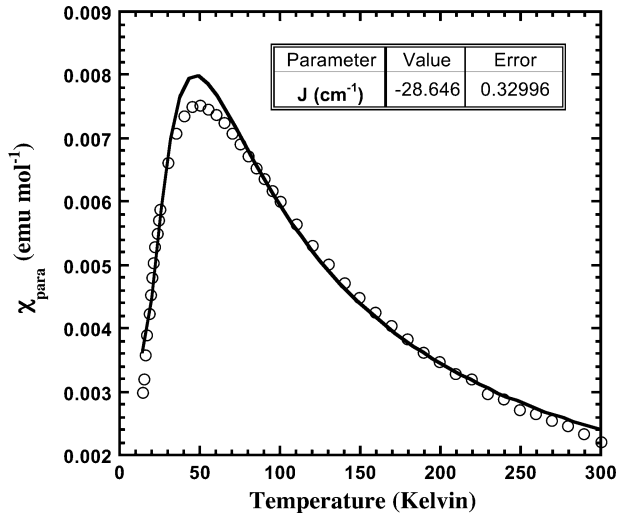

Figure 7. χ_{para} vs T plot for biradical porphyrin **3**.

and $|E/hc| = 0.000\ 23\ cm^{-1}$. From a point dipole model, an interelectronic separation of ca. 9 Å is estimated,[67] slightly greater than the 6.94 Å separation between *meso*-carbons but less than the 12.7 Å distance between SQ ring centers (as determined from the crystal structure).

A Curie plot for the doubly integrated $\Delta m_s = 2$ signal of **3** is shown in Figure 6. The biradical gives a nonlinear response, consistent with $J < 0$ (antiferromagnetic coupling).[68] The data were fit to eq 1:[68,69]

$$I_{EPR} = \frac{C}{T}\left[\frac{3\exp\left(\frac{-2J}{RT}\right)}{1+3\exp\left(\frac{-2J}{RT}\right)}\right] \quad (1)$$

where C is a constant and J is the exchange parameter ($2J$ is the singlet−triplet gap). Best fit results give $J = -75 \pm 3\ cm^{-1}$ for **3**.

Solid-State Magnetic Susceptibility Measurements. The magnetic susceptibility data for **3** are shown in Figure 7 as the molar paramagnetic susceptibility (χ_{para}) versus the temperature. Modeling the temperature-dependent χ_{para} of $S = 1$ molecules can be achieved by fitting to a field-independent van Vleck expression (in this case, a spin dimer model), eq 2,[69,70]

$$\chi_{para} = \frac{2Ng^2\beta^2}{kT[3+e^{-2J/kT}]} \quad (2)$$

where N is Avogadro's number, g is the isotropic Landé factor ($g = 2.0023$), β is the Bohr magneton, T is the temperature in Kelvin, k is Boltzmann's constant, and J is the intramolecular SQ−SQ exchange coupling parameter. The relative singlet- and triplet-state energies were derived using the Hamiltonian, $H = -2J\hat{S}_1\cdot\hat{S}_2$, where $\hat{S}_1$ and $\hat{S}_2$ are the spin operators for the SQs.

The curve fit result gives $J = -29\ cm^{-1}$ and is consistent with an antiferromagnetically coupled dimer. The inclusion of a weak intermolecular term (zJ') did not significantly improve either the quality of the fit or the fit parameters. The χ_{para} versus T plot displays a signature maximum with $T_{max} = 1.285J/k$.[70] The J value from the fit ($-29\ cm^{-1}$) compares well with the value of J determined from T_{max} ($J = -27\ cm^{-1}$).

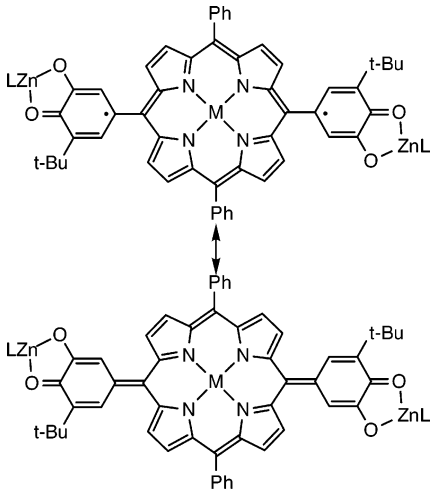

Figure 8. Kekulé resonance structures demonstrating antiferromagnetic SQ−SQ exchange coupling for **3**.

Spin−Spin Coupling in 1−3. The study of spin−spin coupling through nonalternate π systems is an unexplored topic compared to studies of other (alternate) coupler groups. In the present case, the moderately strong antiferromagnetic coupling for **3** is easily explained by the resonance forms shown in Figure 8.Indeed, similar, though less-important, resonance forms predict antiferromagnetic coupling in **1** and **2** as well. The utility of such antiferromagnetically coupled structures lies in part in the possibility of coupling each of the radical spins with a porphyrin-bound *paramagnetic* metal ion. In this way, ground-state $S \neq 0$ molecules can be prepared, regardless of the sign of the metal−radical coupling, if metal−radical coupling exceeds radical−radical coupling, that is, $|J_{M-rad}| > |J_{rad-rad}|$.

Iwamura and co-workers have reported radical-substituted porphyrins topologically similar to **1**−**3** in that zinc was the

(67) Keana, J. F.; Dinerstein, R. J. *J. Am. Chem. Soc.* **1971**, *93*, 2808−2810.
(68) Berson, J. A. *The Chemistry of the Quinonoid Compounds*; Patai, S. R. Z., Ed.; John Wiley & Sons: New York, 1988; Vol. II, p 482.
(69) Bleaney, B.; Bowers, K. D. *Proc. R. Soc. London, Ser. A* **1952**, *214*, 451−465.
(70) Kahn, O. *Molecular Magnetism*; VCH: New York, 1993.

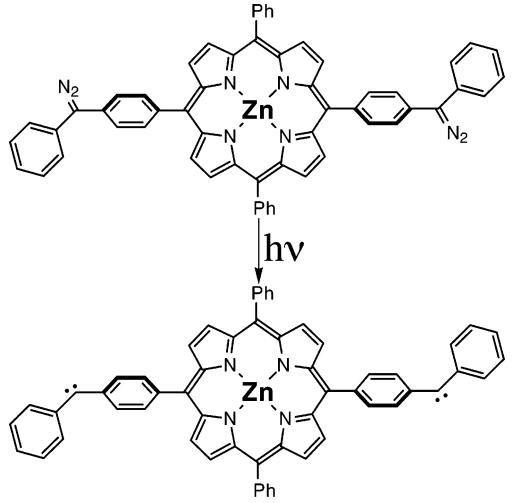

Figure 9. Bis(carbene) Zn^{II} porphyrin prepared by Iwamura and coworkers.

bound metal ion, and the spins were part of delocalized biradicals.[26,27] The spin carriers were diaryl carbenes generated by photolysis of the bis(diazo) precursor, as shown in Figure 9. A J value of -3 cm^{-1} was reported—a significantly weaker antiferromagnetic coupling than that measured for **3**. We propose two mechanisms for weaker coupling in Iwamura's carbene porphyrins. First, it is likely that the meso-aryl carbene groups are unable to relax to a conformation that would maximize spin delocalization into the porphyrin ring following photolysis, and second, the terminal phenyl groups also delocalize spin, thus diluting porphyrin spin density.

Milgrom et al. have shown that the oxidation and subsequent strong antiferromagnetic coupling of *trans*-phenoxyl radicals can give rise to a diamagnetic, quinoidal porphyrin with Ni^{II}, whereas the larger Pd^{II} precludes the requisite ruffled conformation and resists oxidation.[71−74]

Comparison of 1−3. Semiquinones have greater ring spin densities (ca. 0.8) than phenyl-*tert*-butylnitroxides (ca. 0.1−0.15).[38,49,75] Because of the greater spin density near the porphyrin ring, the average interelectronic distance in the bis(SQ)porphyrins is less than that for the bis(nitroxide) porphyrins, and this is manifested in both zero-field splitting and exchange coupling in biradical **3**. Clearly, **3** should be superior to both **1** and **2** for the future construction of magnetic chain coordination polymers.

Conclusions

The bis(nitroxide) porphyrins **1** and **2** exhibit fluid-solution EPR spectra consistent with $|J| \gg |a|$. No evidence was observed for the modulation of J as shown by the temperature invariance of the EPR spectra. Thus, bond rotations in **1** and **2** do not cause $|J|$ to approach the value of $|a|$. Frozen-solution EPR spectra of **1** and **2** do not include a $\Delta m_s = 2$ transition, consistent with weak zero-field splitting due to limited interaction of the nitroxide moieties. Thus, exchange coupling in the bis(nitroxide) porphyrins is weak and apparently not differentially modulated by C=C and C≡C—at least according to EPR spectroscopic measurements.

The frozen-solution EPR spectrum of **3** exhibits zero-field splitting and a $\Delta m_s = 2$ transition characteristic of a triplet state. The intensity of the $\Delta m_s = 2$ transition of **3** was measured as a function of temperature, and the data were fit according to a singlet−triplet model to yield $J = -75$ cm^{-1}—a substantial exchange parameter considering the size of the porphyrin π system through which coupling occurs. Consistent with the π topology, the exchange parameter is antiferromagnetic. This interaction is substantially greater than that between phenylcarbene units through the porphyrin π system measured by Iwamura's group ($J = -3$ cm^{-1}).[26,27] In the latter case, the carbene units were generated from a bis(diazo) precursor in which porphyrin−phenyl torsion minimized carbene conjugation with the porphyrin ring, and the second phenyl group attached to the carbene delocalized some of the π spin density. Both of these effects would serve to attenuate the exchange interaction between the carbene units. In the solid state, the exchange parameter ($J = -29$ cm^{-1}) is attenuated compared to the value obtained from fitting the EPR spectral intensity data. Because we have shown that the exchange coupling in π-type biradicals varies with the cos^2 of the torsion angles,[45,49] the stronger frozen-solution coupling suggests that the frozen-solution structure(s) have smaller SQ−porphyrin torsion angles that permit greater SQ spin delocalization.

The utility of antiferromagnetically coupled biradicals **1**−**3** lies in the possibility of ferromagnetically coupling each of the radical spins with a bound paramagnetic metal ion. In this way, overall ferromagnetic alignment might be achieved. The present results represent the first examples of stable radicals exchange-coupled through a porphyrin π system and, for **3**, the first structurally characterized example of such. Porphyrins **1**−**3** also complement the studies of exchange-coupled porphyrin dimers.[31−35] Future efforts will focus on coordination polymers of these biradical ligands.

Experimental Section

Chemicals were purchased from Aldrich Chemical Co. unless noted otherwise. Solvent distillations, synthetic procedures, and electrochemistry were carried out under an argon atmosphere. Tetrahydrofuran (THF) was distilled from sodium benzophenone-ketyl prior to use. Methylene chloride was distilled from calcium hydride. X-band EPR spectra were recorded on an IBM-Brüker E200SRC spectrometer fitted with an Oxford model 900 cryostat. Radical formation was accomplished as reported previously.[40] Magnetic susceptibilities were measured on a Quantum Design MPMS-XL7 SQUID magnetometer using an applied field of 1 T for Curie plots. Data for crystalline samples were corrected for molecular diamagnetism using Pascal's constants. Microcrystalline

(71) Milgrom, L. R.; Yahioglu, G.; Jogiya, N. N. *Free Radical Res.* **1996**, *24*, 19−29.
(72) Golder, A. J.; Milgrom, L. R.; Nolan, K. B.; Povey, D. C. *J. Chem. Soc., Chem. Commun.* **1989**, 1751−1753.
(73) Golder, A. J.; Milgrom, L. R.; Nolan, K. B.; Povey, D. C. *J. Chem. Soc., Chem. Commun.* **1987**, 1788−1790.
(74) Milgrom, L. R. *Tetrahedron* **1983**, *39*, 3895−3898.
(75) Forrester, A. R.; Hay, J. M.; Thompson, R. H. *Organic Chemistry of Stable Free Radicals*; Academic: London, 1968.

samples were loaded into the sample space of a Delrin sample holder and mounted directly to the sample rod. The sample holder was subtracted out using an empty Delrin sample holder as the background.

Porphyrin 1(TBS)$_2$. A 100 mL flask containing 4-[N-*tert*-butyl-N-(*tert*-butyldimethylsilyloxy)amino]phenyl-1-boronic acid pinacol ester (1.07 g, 2.99 mmol), **4** (0.765 g, 1.19 mmol), $Pd(PPh_3)_4$ (0.0828 g, 0.072 mmol), and Na_2CO_3 (2M, 3 mL) in THF (50 mL) was pumped and purged under N_2 five times. The reaction mixture was refluxed for 2 days. Once cool, the solvent was removed under reduced pressure, and ether was added, and then, the reaction mixture was filtered to remove the inorganic salt. The remaining crude mixture was purified by an alumina column with 10−30% CH_2Cl_2/petroleum ether and chromatotran with 30% CH_2Cl_2/petroleum ether to give the first band, free-base **1(TBS)$_2$** (0.449 g, 37%), and the second band, **1(TBS)$_2$** (0.515 g, 40%). Free-base **1(TBS)$_2$**. ^{1}H NMR ($CDCl_3$, δ): 8.86 (d, 8H, J = 4.4 Hz), 8.23 (d, 4H, J = 7.6 Hz), 8.08 (d, 4H, J = 8.4 Hz), 7.76 (d, 6H, J = 5.6 Hz), 7.64 (d, 4H, J = 7.2 Hz), 1.37 (s, 18H), 1.05 (s, 18H), 0.15 (s, 12H), −2.74 (s, 2H). ^{13}C NMR ($CDCl_3$, δ): 151.1, 142.4, 138.6, 134.8, 133.8, 131.3, 131.2 (broad), 127.9, 126.8, 123.8, 120.3, 120.2, 61.3, 26.6, 26.5, 18.4, −4.3. IR (film from $CDCl_3$): 3306.4, 2920.4, 2849.8, 1555.7, 1463.8, 1351.9, 1246.3, 1193.0, 935.3, 855.1, 832.2, 793.3, 697.1, 665.3 (cm^{-1}). MS−FAB $C_{64}H_{76}O_2N_6Si$ calcd exact mass: 1016.5568. Observed: 1016.5594. **1(TBS)$_2$**. ^{1}H NMR ($CDCl_3$, δ): 8.97 (s, 8H), 8.24 (s, 4H), 8.08 (s, 4H), 7.76 (s, 6H), 7.65 (s, 4H), 1.38 (s, 18H), 1.05 (s, 18H), 0.16 (s, 12H). ^{13}C NMR ($CDCl_3$, δ): 150.9, 150.6, 150.4, 143.1, 139.2, 134.8, 134.6, 133.6, 132.1, 127.7, 126.7, 123.7, 121.3, 61.3, 26.6, 26.5, 18.4, −4.3. IR (film from $CDCl_3$): 2956.2, 2855.2, 1646.0, 1487.8, 1337.8, 1249.1, 1202.0, 1070.2, 998.4, 942.5, 909.0, 858.0, 833.2, 781.2, 706.1, 666.6 (cm^{-1}). MS−FAB $C_{64}H_{74}O_2N_6SiZn_2$ calcd exact mass: 1078.4703. Observed: 1078.4681.

Porphyrin 1. The TBS-protected porphyrin was deprotected and oxidized as described previously.[38] Anal. Calcd for $C_{52}H_{44}N_6O_2$: C, 79.56; H, 5.64. Found: C, 79.22; H, 5.44.

Porphyrin 2(TBS)$_2$. A 100 mL flask containing 4-trimethylsilanylethylnyl-1-[N-*tert*-butyl-N-(*tert*-butyldimethylsilyloxy)amino]-benzene (0.535 g, 1.423 mmol), **5-Zn** (0.332 g, 0.485 mmol), K_2CO_3 (0.295 g, 2.130 mmol), piperidine (0.96 mL, 9.70 mmol), $Pd(PPh_3)_4$ (56 mg, 0.049 mmol), CuI (5.0 mg, 0.024 mmol), THF (30 mL), and distilled methanol (4 mL) was pumped and purged 10 times and then refluxed for 58.5 h. Once cool, saturated NH_4Cl was added. The organic layer was washed with ether twice separated, and dried over Na_2SO_4, and the solvent was removed in vacuo. The mixture was purified by flash chromatography (alumina, 20% CH_2Cl_2/petroleum ether for the first and second bands, 90% CH_2Cl_2/petroleum ether for the third band, and 100% CH_2Cl_2), giving **2(TBS)$_2$** (0.2560 g, 47% yield).^{1}H NMR ($CDCl_3$, δ): 9.70 (d, 4H, J = 4.7 Hz), 8.86 (d, 4H, J = 4.7 Hz), 8.18 (d, 4H, J = 7.1 Hz), 7.91 (d, 4H, J = 8.4 Hz), 7.79 (d, 6H, J = 5.8 Hz), 7.47 (d, 4H, J = 7.9 Hz), 1.23 (s, 18H), 1.00 (s, 18H), 0.01 (s, 12H). ^{13}C NMR ($CDCl_3$, δ): 152.2, 152.1, 150.2, 142.4, 134.6, 132.8, 131.2, 131.0, 127.8, 126.9, 125.6, 122.9, 120.3, 102.3, 97.4, 92.1, 61.6, 26.5, 26.4, 18.3, −4.3. IR (film from CH_2Cl_2): 2956.9, 2928.1, 2855.7, 1598.1, 1498.4, 1461.8, 1359.9, 1256.1, 1206.9, 1002.1, 943.5, 859.8, 834.0, 781.6, 701.4 (cm^{-1}). MS−FAB $C_{68}H_{76}O_2N_6Si_2Zn_2$ calcd exact mass: 1126.4703. Observed: 1126.4718.

Porphyrin 2. The TBS-protected porphyrin was deprotected and oxidized as described previously.[38] Anal. Calcd for $C_{56}H_{44}N_6O_2$: C, 80.74; H, 5.32. Found: C, 80.32; H, 5.29.

5',15'-Bis-[3,4-di-(methoxymethoxy)-5-*tert*-butyl]phenyl-10',20'-di-phenylporphyrin 3(MOM)$_4$. A 50 mL Schlenk flask containing 3,4-[di-methoxymethoxy]-5-*tert*-butyl-phenyl-1-boronic pinacol ester (0.268 g, 0.805 mmol), 5′,15′-di-bromo-10′,20′-diphenylporphyrin (0.178 g, 0.287 mmol), $Pd(PPh_3)_4$ (0.033 g, 0.029 mmol), Na_2CO_3 (2M, 0.7 mL) in ethanol (0.5 mL), and THF (8 mL) was pumped and purged under N_2 seven times. The reaction mixture was refluxed for 2 days. Once cool, the solvent was removed under reduced pressure. The crude material was diluted with ether and filtered through a pad of Celite to remove the inorganic salts. The remaining crude mixture was purified by radial chromatagraphy using 4−10% THF/petroleum ether. The collected fraction was a dark purple solid, **3(MOM)$_4$** (0.150 g, 54%). ^{1}H NMR (CDCl3, δ): 8.93 (d, 4H, J = 4.3 Hz), 8.85 (d, 4H, J = 4.3 Hz), 8.22 (d, 4H, J = 6.2 Hz), 7.91 (d, 4H, J = 11.6 Hz), 7.76 (d, 6H, J = 6.1 Hz), 5.55 (s, 4H), 5.35 (s, 4H), 3.83 (s, 6H), 3.56 (s, 6H), 1.60 (s, 18H), −2.78 (s, 2H). MS−FAB $C_{66}H_{62}N_4O_8$ calcd exact mass: 966.4568. Observed: 966.4581.

Porphyrin 3. To a 25 mL round-bottom flask was added **3-(MOM)$_4$** (0.078 g, 0.08 mmol), two drops of concentrated HCl, and MeOH (10 mL). The reaction mixture was purged several times with N_2 and set to reflux for 12 h. After cooling, the MeOH was removed under reduced pressure. The crude reaction mixture was diluted with CH_2Cl_2 and washed with NH_4Cl (1 × 15 mL) and brine (3 × 15 mL), dried over Na_2SO_4, and filtered, and the solvent was removed in vacuo. The purple solid was purified by a pentane wash. This gave 0.062 g (97% yield) of the free-base bis(catechol)-porphyrin as a purple crystalline solid. ^{1}H NMR (300 MHz, d_6-acetone, δ): 9.05 (d, 4H, J = 4.0 Hz), 8.88 (d, 4H, J = 3.9 Hz), 8.28 (s, 4H), 7.87 (d, 6H, J = 3.4 Hz), 7.73 (d, 4H, J = 7.3 Hz), 7.64 (s, 2H), 1.66 (s, 18H), −2.46 (s, 2H). ^{13}C NMR (d_6-acetone, δ): 148.4, 145.9, 142.4, 141.4, 136.9, 134.5, 131.1, 128.1, 127.7, 126.7, 121.7, 120.2, 120.1, 22.9.

The product was placed in a 50 mL round-bottom flask, and $Zn(OAc)_2 \cdot H_2O$ (0.188 g, 0.857 mmol), EtOH (1 mL), and distilled THF (25 mL) were added. The reaction was stirred under N_2 and reflux conditions for 3 h. After cooling, the solvent was removed under reduced pressure. The crude reaction mixture was diluted with CH_2Cl_2 and washed with brine (2 × 20 mL) and distilled H_2O (1 × 15 mL), dried over Na_2SO_4, and filtered, and the solvent was removed in vacuo. The crude product was washed with pentane. This yielded a purple solid (0.065 g, 97%). ^{1}H NMR (300 MHz, d_6-acetone, δ): 9.08 (d, 4H, J = 4.5 Hz), 8.90 (d, 4H, J = 4.6 Hz), 8.2 (d, 4H, J = 2.3 Hz), 7.83 (d, 6H, J = 2.8 Hz), 7.72 (d, 4H, J = 10.2 Hz), 1.66 (s, 18H).

The product was placed in a 25 mL round-bottom flask containing $Tp^{Cum,Me}ZnOH$ (0.112 g, 0.162 mmol) in a mixture of MeOH (5 mL) and CH_2Cl_2 (5 mL) and was stirred overnight in the air. The reaction mixture was concentrated by rotary evaporation and washed with cold MeOH. The reddish-brown precipitate was collected by filtration and then recrystallized from 1:1 CH_2Cl_2/pentane. IR (film from CH2Cl2) ν (cm^{-1}): 2924, 2546, 1574, 1551, 1519, 1441, 1362, 1262, 1186, 1066, 836, 794, 746, 701. UV−vis λ_{max} (nm): 418, ϵ ($M^{-1}cm^{-1}$) = 96 074. MS−FAB $C_{130}H_{132}N_{16}O_4B_2Zn_3$ calcd exact mass: 2194.87. Observed: 2195.02.

Acknowledgment. This work was funded by the National Science Foundation (CHE-0091247 and CHE-0345263). Mass spectra were obtained at the Mass Spectrometry Laboratory for Biotechnology. Partial funding for the facility

was obtained from the North Carolina Biotechnology Center and the National Science Foundation. The MALDI-TOF mass spectrometer was funded in part by the North Carolina Biotechnology Center.

Supporting Information Available: X-ray crystallographic files for **3** in CIF format and relevant crystallographic data. This material is available free of charge via the Internet at http://pubs.acs.org.

IC060209Z